DOI 10.1007/s10891-022-02618-4
Journal of Engineering Physics and Thermophysics, Vol. 95, No. 6, November, 2022

CONJUGATE NONSTATIONARY HEAT TRANSFER IN THE COURSE OF SUPERSONIC SPATIAL FLOW PAST A SPHERICALLY BLUNTED CONE MADE FROM A COMBINED MATERIAL

V. I. Zinchenko and V. D. Gol'din

UDC 536.245

The flow at different angles of attack past a spherically blunted cone, the spherical and conical parts of which are made of different materials is considered. It is shown theoretically that the manufacture of the side surface of such a body from a highly thermally conductive material provides heat removal from its spherical part, which experiences maximum thermal loads and, accordingly, a decrease in the maximum body temperatures in this area. Dimensionless expressions are obtained for estimating the decrease in the maximum temperatures of a conical body in the area of its spherical bluntness, when the body is immersed in a flow at different angles of attack, by choosing the geometry of the body and materials that have the necessary thermophysical characteristics to cover it.

Keywords: *supersonic flow, aerodynamic heating, conjugate heat transfer, angle of attack, heat-shielding materials, laminar boundary layer.*

Introduction. This work is a continuation of works [1, 2], in which the efficiency of thermal protection of a spherically blunted cone immersed in a gas flow moving with supersonic and hypersonic velocities was investigated. To create such protection the most promising is the manufacture of coating from a high-temperature material on the frontal part of a body, which is immersed in a flow and which is subjected to maximum thermal loads, with the lateral surface of the body being made of a highly thermally conductive material that provides heat removal from the frontal part of the body to the area where its heat fluxes $q_w(\xi, \eta)$ are relatively low. When a body moves at an angle of attack, the flow of heat in its coating material in the longitudinal and circumferential directions, as well as heat reradiation by the body surface can lead to a noticeable decrease in the maximum temperatures of the frontal part of the body.

Combinations of materials for the front and side parts of the body immersed in a flow were investigated experimentally and theoretically in many works. In [3–7], the behavior of ultrahigh-temperature materials was studied when they were passed over by supersonic axisymmetric jets generated by a plasmatron. In the general case of flow around a body at an angle of attack, it is necessary to consider three-dimensional conjugate heat exchange between the body and gas in the boundary layer and heat propagation in the combined material of the body with the corresponding boundary and initial conditions [8, 9].

In this paper, the term combined material of a conical spherically blunted body is used to denote the fact that the frontal and lateral parts of the body are made of different materials. The aim of this work is to compare the effectiveness of using various materials, both simple and complex, to provide thermal protection for such a body, as well as to obtain dimensionless relations for engineering estimates of the maximum temperatures of its frontal part.

Formulation of the Problem. As in [1], the flow past a spherically blunted cone with half-angle (3, spherical bluntness radius R_n, and length $z_c = 10$ at the angle of attack α is considered. In contrast to [1], the frontal part of the conical body is made of material 1, and there is a conical shell of constant thickness $L = 0.5$ made of material 2 on its lateral part ($z > z_0$) (all linear dimensions are related to R_n). The scheme of the computational domain is shown in Fig. 1.

Under the assumptions made, the spatial boundary layer on the surface of a conical body is described by the system of equations in Dorodnitsyn-Lees variables presented in [1], The thermal field inside the heat-shielding shell of the body, the thermal conductivity of which materials is assumed to be constant, is described by the following system of heat conduction equations in a dimensionless form:

Tomsk State University, 36 Lenin Ave., Tomsk, 634050, Russia; email: vdg@math.tsu.ru. Translated from Inzhenerno-Fizicheskii Zhurnal, Vol. 95, No. 6, pp. 1526-1536, November-December, 2022. Original article submitted May 27, 2021.

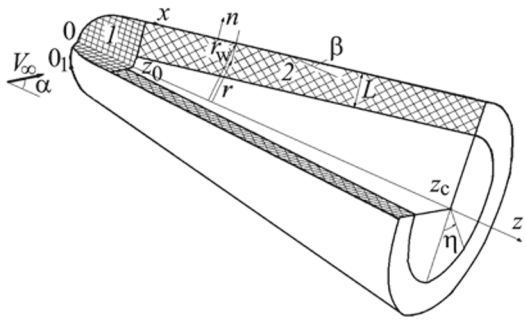

Fig. 1. Scheme of the computational domain.

$$\frac{1}{S_1}\frac{\partial\theta_1}{\partial\tau} = \frac{1}{r}\frac{\partial}{\partial r}\left(r\frac{\partial\theta_1}{\partial r}\right) + \frac{\partial^2\theta_1}{\partial z^2} + \frac{1}{r^2}\frac{\partial^2\theta_1}{\partial\eta^2}\,, \tag{1}$$

$$\frac{1}{S_2}\frac{\rho_{s2}c_{s2}}{\rho_{s1}c_{s1}}\frac{\partial\theta_2}{\partial\tau} = \frac{1}{r}\frac{\partial}{\partial r}\left(r\frac{\partial\theta_2}{\partial r}\right) + \frac{\partial^2\theta_2}{\partial z^2} + \frac{1}{r^2}\frac{\partial^2\theta_2}{\partial\eta^2}\,, \tag{2}$$

where $\theta_i = \dfrac{T_i}{T_{e0}}$, $S_i = \dfrac{\lambda_{si}}{\sqrt{\rho_{e0}\mu_{e0}V_{max}R_n}}\dfrac{T_{e0}}{h_{e0}}$, $\tau = \dfrac{\lambda_{s1}t}{\rho_{s1}c_{s1}R_n^2}\dfrac{1}{S_1}$, and $V_{max} = \sqrt{2h_{e0}}$. At the initial instant of time the body temperature is set:

$$\theta(0,\, r,\, z,\, \eta) = \theta_{in} = \frac{T_{iin}}{T_{e0}}\,. \tag{3}$$

As boundary conditions for Eqs. (1) and (2) on the symmetry axis of the body, as well as on the inner and back surfaces of its shell, the thermal insulation conditions are assigned:

$$\partial\theta_i/\partial n = 0\,, \tag{4}$$

where differentiation is carried out along the normal to the corresponding surface. At the boundary of regions 1 and 2 the conjugation conditions are used. Boundary conditions of the 4th kind are set at the interface between the gaseous and solid phases, i.e., the equality of temperatures and heat fluxes in the boundary layer and in the solid body is assumed:

$$\tilde{q}_w - \pi_\sigma\theta_{wi}^4 = -S_i\frac{\partial\theta}{\partial n_1}\,. \tag{5}$$

Here $\pi_\sigma = \dfrac{\varepsilon\sigma T_{e0}^4\sqrt{R_n}}{h_{e0}\sqrt{\rho_{e0}\mu_{e0}V_{max}}}$ and $\tilde{q}_w = \dfrac{q_w}{q_w^*}$ is the dimensionless heat flux from the boundary layer, where $q_w^* = \sqrt{\dfrac{\rho_{e0}\mu_{e0}V_{max}}{R_n}}\,h_{e0}$ is characteristic value of the heat flux q_w.

In the Dorodnitsyn–Lees variables $\left(\xi = \dfrac{x}{R_n} \text{ and } \zeta = \dfrac{u_e r_w}{\sqrt{2R_n\int\limits_0^\xi \rho_e\mu_e u_e r_w^2 d\xi}}\int\limits_0^0 \rho dn\right)$ for the dimensionless heat flux the following relation holds:

$$\tilde{q}_w = \sqrt{\frac{u_e}{V_{max}}\frac{\rho_e}{\rho_{e0}}\frac{\mu_e}{\mu_{e0}}\frac{1}{\alpha_1}}\left(\frac{l}{\mathrm{Pr}}\frac{\partial g}{\partial\zeta}\right)_w\,,$$

TABLE 1. Thermophysical Characteristics of Materials

Material	λ_s, W/(m·K)	ρ_s, kg/m^3	c_s, J/(kg·K)
Steel	20	7800	600
Aluminum alloy	240	2300	1000
Copper	386	8950	370
Aluminum–magnesium alloy	120	2300	1000

where $\alpha_1 = \dfrac{2\int_0^{\xi} \rho_e \mu_e u_e r_w^2 d\xi}{\rho_e \mu_e u_e r_w^2}$, $l = \dfrac{\mu\rho}{\mu_e \rho_e}$, and Pr is the Prandtl number equal to 0.72 for air.

The solution of the heat conduction equations for the body is determined for the most part by the parameters of the conjugacy of its parts S_i and by the parameter π_σ characterizing the radiation of heat by the body surface. In the limiting case of $S_i = 0$, the solution of the system of equations for hydrodynamic boundary layer with the boundary condition (5) gives the distribution of the radiation-equilibrium temperature on the body surface $\theta_{w,r}(\xi, \eta)$. The case $S_i \to \infty$ co corresponds to materials with infinite thermal conductivity, with the body temperature being dependent only on time [10]. Studying the motion of a body at an angle of attack in these two limiting cases makes it possible to estimate the possible decrease in the maximum temperature of the body due to the choice of a material for covering it with certain thermophysical characteristics (the thermal conductivity of the material is especially important).

Technique of Solving the Problem and Initial Data. The technique of solving the boundary-value problem of conjugate heat transfer between a spherically blunted cone and a spatial gas flow past it was given in [1]. In the present work, we determine the temperature field in the body at different values of the coefficients λ_{si} in regions 1 and 2.

In the calculations, by analogy with [1], we used the following input data: $M_\infty = 6.1$, $pe0 = 2.2$ bar, $T_{w,in} = 293$ K, $\varepsilon = 0.8$, $L = 0.5$, $z_0 = 1.5$, and $\beta = 10^o$. We investigated the effect of the geometric parameters of a conical body and of the surface gas stagnation temperature on the temperature inside the body. Calculations were carried out for $R_n \sim 0.004$ m, $T_{e0} = 1500$ and 2000 K. The thermophysical characteristics of the investigated materials of the body are given in Table 1. In general, for different conditions of solving the problem in the conjugate formulation, the evolution of the three-dimensional temperature field inside the body depending on the time of heating the body and its materials was observed.

An Example of Solving the Problem in a Conjugate Formulation. Figures 2–5 present the results of solving the problem of conjugate nonstationary heat exchange between a spherically blunted conical body and a supersonic gas flow past it at an angle of attack, depending on the properties of the body material at $T_{e0} = 1500$ K and $R_n = 0.004$ m. Figure 2 shows the temperature distributions over the body surface in the plane of symmetry of the flow at different angles of attack. The point of intersection of the surface of the frontal part of the body with the axis of its symmetry was chosen as the origin of the coordinate system. It follows from Fig. 2 that during the flow past the body at zero angle of attack the selected combined materials provide equalization of the temperature fields $T_w(\xi)$ on the surface of the conical part of the body in almost the entire range of the time of the body flight. In the case of a stationary flow past the body, due to the flow of heat from its spherical part to the conical one, the use of combined highly heat-conductive materials reduces the maximum temperature of the body surface in the vicinity of the flow stagnation point by about 50 K in comparison with a homogeneous material (steel). The maximum temperature on the side surface of the windward part of the body decreases by approximately the same value at an angle of attack of 10^o (Fig. 2c). In this case, the use of combined highly heat-conductive materials for fabricating the surface of the remote leeward part of the body leads to an increase in its temperature by 100 K compared to steel (curve 2). Under stationary conditions, for all considered bodies with combined materials immersed in a flow at different angles of attack the temperatures of the windward and leeward sides of their lateral conical surface are equalized. At the same time, the spherical part of the body is characterized by a decrease in maximum temperatures, as in the case of a zero angle of attack. As the same time, for a homogeneous material consisting of poorly conducting steel (curves 2), with an increase in the angle of attack, the difference in the temperatures of the windward and leeward surfaces of the conical part of the body increases, which is determined by the behavior of heat fluxes $q_w(\xi, \eta)$. This is especially

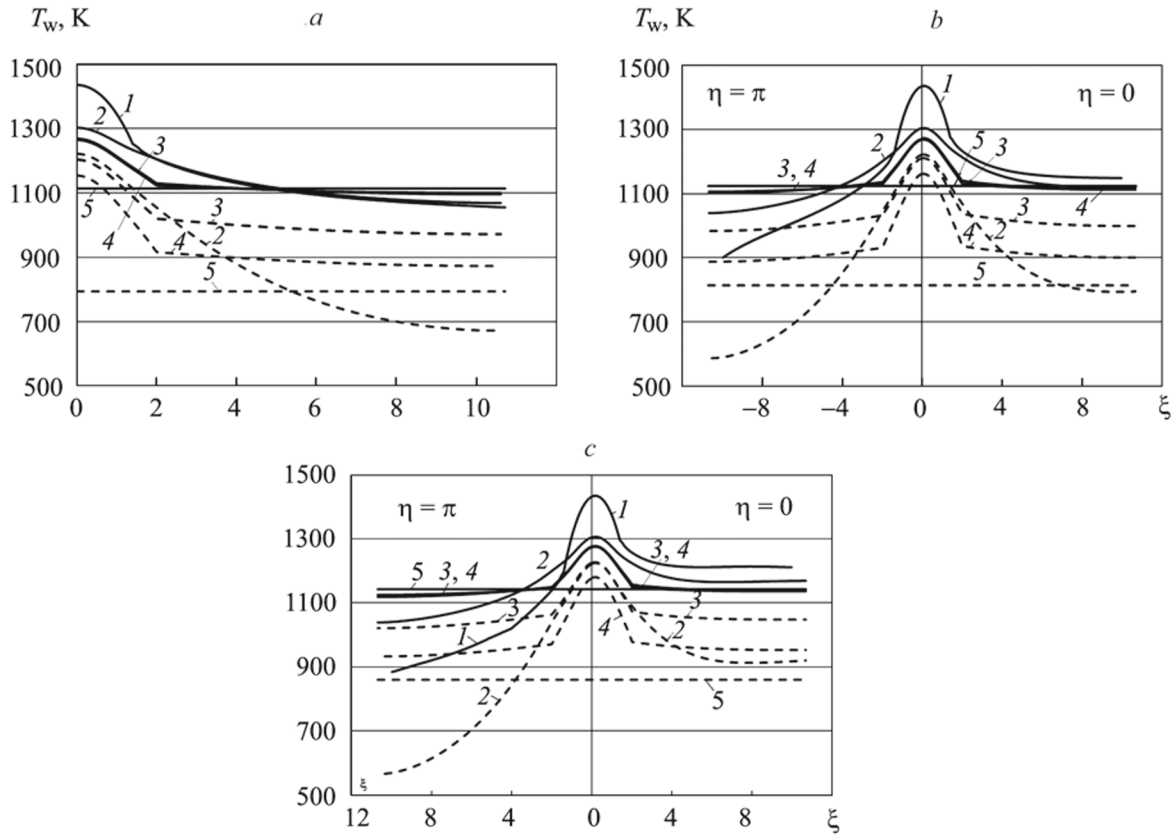

Fig. 2. Temperature distribution over the surface of spherically blunted conical bodies made of steel (2), steel + aluminum alloy (3), steel + copper (4), and a material with infinite thermal conductivity (5) immersed in a flow at angles of attack $\alpha = 0$ (a), 5 (b), and 10^o (c): 1) radiation equilibrium temperature; solid lines, stationary values of parameters; dashed lines, the values of parameters at $t = 20$ s.

pronounced in the region of nonstationary heating of the body, which confirms the possibility of effective control of its temperature regime by respective selection of a combined material.

Typical behavior of the quantity T_{w0} depending on time is shown in Fig. 3 for the angle of attack $\alpha = 10^o$. Note that at all angles of attack in the vicinity of the critical point, the stationary temperatures for a homogeneous material (steel) have close values, and, when using a combined material, T_{w0} takes on lower values. The temperature dependences $T_w(t)$ in the vicinity of the plane of symmetry on the windward and leeward sides of the body at $\xi = 8.7$ (dashed-dotted and dashed lines, respectively) illustrate close values of temperatures in using combined materials with some increase in the temperature on the windward side of the body over the entire range of the times of the process. In this case, for a conical surface the values of λ_s determine the value of $\partial T_w/\partial t$. When the stationary mode of heat transfer is reached, the temperatures of the conical surface of the body in the planes of its symmetry are close for both combined materials, as was noted in the analysis of Fig. 2.

Figure 4 shows distributions of relative Stanton numbers $\dfrac{\mathrm{St}(\xi, \eta)}{\mathrm{St}_0} = \dfrac{\tilde{q}_w(\xi, \eta)}{\tilde{q}_w(0)} \dfrac{1 - \theta_{w0}}{1 - \theta_w(\xi, \eta)}$ on the spherical and conical parts of the body in a flow at an angle of attack $\alpha = 0^o$, as well as in the vicinity of the flow symmetry plane for $\alpha = 10^o$ at the initial instant of time (curves 1) and when the heat transfer process reaches the stationary regime (curves 2–4). As follows from this figure, in the peripheral area of the spherical part of the body the ratio $\mathrm{St}/\mathrm{St}_0$ in the stationary case is smaller by 40–50% in comparison with the initial distribution of the relative Stanton numbers. At the same time, as $\tau \to \infty$, the influence of the material of the body in a flow on this ratio is much weaker. In the case of a zero angle of attack, the values of the ratio $\mathrm{St}/\mathrm{St}_0$ on the lateral conical surface of the body at $\tau = 0$ and $\tau \to \infty$ are close enough (Fig. 4a), and at $\alpha = 10^o$ the values of the indicated ratio on the windward and leeward sides of the body in the vicinity of the plane of its

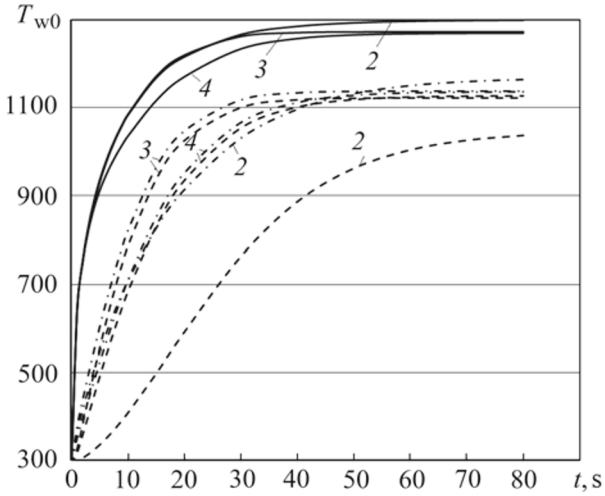

Fig. 3. Changes in time of the surface temperatures of bodies made of steel (2), steel + aluminum alloy (3), steel + copper (4), and a material with infinite thermal conductivity (5) immersed in a flow at an angle of attack $\alpha = 10^{o}$, at the critical point (solid lines), the point $\xi = 8.7$ on the leeward side of the body (dashed lines), and at the point $\xi = 8.7$ on its windward side (dash-dotted lines).

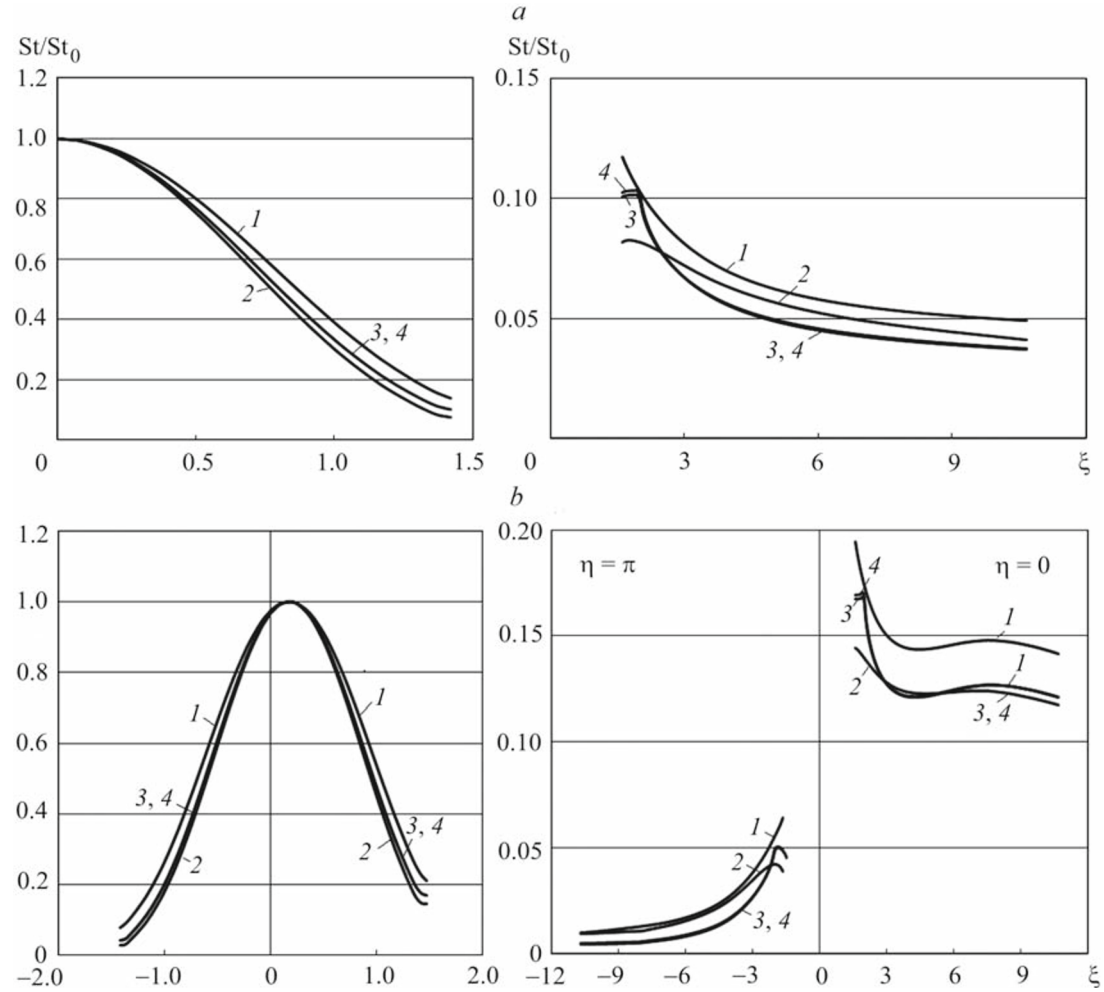

Fig. 4. Distribution of Stanton numbers on the spherical and conical parts of bodies made of steel (2), steel + aluminum alloy (3), and steel + copper (4) immersed in a flow at angles of attack $\alpha = 0$ (a) and 10^{o} (b): 1) initial instant of time; 2–4) stationary distributions.

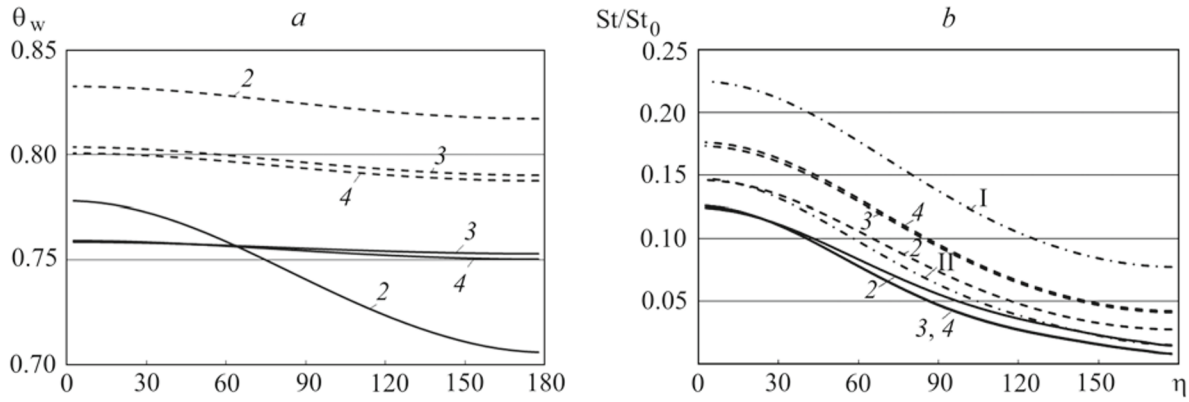

Fig. 5. Distributions of dimensionless temperature (a) and of relative Stanton numbers (b) along the circumferential coordinate on the surface of bodies made of steel (2), steel + aluminum alloy (3), steel + copper (4), and a material with infinite thermal conductivity (5) immersed in a flow at an angle of attack $\alpha = 10^{o}$ at the points $\xi = 1.42$ (dashed lines) and 7 (solid lines); dash–dotted lines, data for the points $\xi = 1.42$ (I) and 7 (II) at the initial instant of time.

symmetry can differ by a factor of 10 in the stationary mode of heat transfer with a weak effect of the temperature of the body surface on this difference regardless of the body material. As shown in [1], the above estimates can increase noticeably at the nonstationary stage of heating the body, where the nonmonotonic behavior of the ratio St/St_0 depending on time is observed. The calculations performed in this work showed that at $\alpha = 10^{o}$ the maximum difference of the values of St/St_0 on the windward and leeward sides of the body reaches 20 and occurs at $\tau \approx 8$.

Figure 5 gives an idea of the distribution of temperatures and heat fluxes along the circumferential coordinate on the body surface. It should be noted that at the accepted input data, the results obtained agree qualitatively, and some of them quantitatively, with the distributions of θ_w and St/St_0 presented in Fig. 7 in [1], Taking into account the equalization of θ_w along the circumferential coordinate in the stationary case (curves 3 and 4 in Fig. 5a), the relative numbers $St/St_0(\eta)$ coincide on the conical part of the body for different materials (lines 3 and 4 in Fig. 5b). This fact can be used for estimating the heat transfer coefficients on the surface of the conical part of bodies made of combined materials in the stationary case, including the limiting case of an isothermal surface (lines 5 in Fig. 2).

Generalized Results of Solving the Problem in a Dimensionless Form. *Stationary case.* Comparing the development of thermal regimes of combined and homogeneous bodies, an important point is the possibility of replacing combined bodies with homogeneous ones made of materials with effective characteristics. Such an approach can provide technological advantages and optimization of the characteristics of a body immersed in a flow. Since the maximum heat fluxes and temperatures on its surface are reached in the vicinity of the frontal critical point in laminar flow past a spherically blunted conical body, we will first consider this region. As follows from [1], the maximum body temperature depends weakly on the angle of attack, so we first consider the flow past the body at a zero angle of attack.

Figure 6a presents the dependences of the dimensionless temperature at the critical point Owo and of the quantity

$$\varphi_{st} = \frac{\theta_{w,r} - \theta_{w0}}{\theta_{w,r} - \theta_w(\lambda_s \to \infty)} \tag{6}$$

on the number S for homogeneous materials. Next, calculations of combined bodies were carried out and the corresponding values of θ_{w0} were found. For these values we selected the effective values of the parameter S_{eff} of homogeneous bodies that provide the same values of θ_{w0}. Thus, effective homogeneous bodies were selected instead of combined bodies (Fig. 6b). So, according to the solid curve 1, an effective homogeneous body corresponding to a combined steel + aluminum–magnesium (AMG) body has $S_{eff} = 2.02$ at parameters providing $\theta_{w0} = 0.850$. For the steel + copper body $S_{eff} = 2.37$ at $\theta_{w0} = 0.843$. According to dashed curve 1, at $\pi_\sigma = 0.09$ and $T_{e0} = 2000$ K for the steel + AMG body $S_{eff} = 1.77$ at $\theta_{w0} = 0.808$ and for the steel + copper body $S_{eff} = 2.05$ at $\theta_{w0} = 9.799$. Note that the value of S_{eff} can be found from the calculated values of θ_{w0}, as well as of φ_{st} (6) calculated using the value of θ_{w0} for an effective homogeneous body with subsequent determination of the

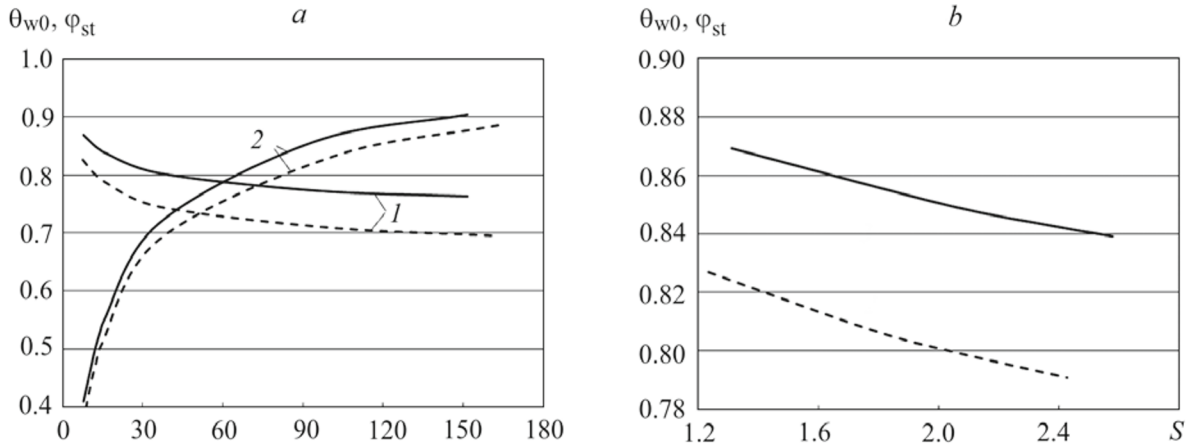

Fig. 6. Dependences θ_{w0} (1) and φ_{st} (2) on the parameter S for homogenous (a) and effective (b) bodies: solid lines, $\pi_\sigma = 0.04$, $T_{e0} = 1500$ K; dashed lines, 0.09, 2000.

conjugation parameter $S = S_{eff}$ with account for the dependences presented in Fig. 6. Thus, the dependences presented in Fig. 6 make it possible to determine the maximum temperature of both homogeneous bodies and combined bodies reduced to effective homogeneous bodies.

Nonstationary case. Let us generalize the problem considered above for stationary conditions in the vicinity of the frontal critical point of a spherically blunted conical body immersed in a flow at a zero angle of attack in the nonstationary case (Fig. 7). To this end, we replace the combined body by a homogeneous body made of a material with effective characteristics.

Using the expression for dimensionless time $\tau = \dfrac{t}{\rho_{s1}c_{s1}R_n^2}\sqrt{\rho_{e0}\mu_{e0}V_{max}R_n}\,\dfrac{h_{e0}}{T_{e0}}$, in which $\rho_{s1}c_{s1}$ relates to steel, for the effective homogeneous body we can write $\tau_{eff} = \dfrac{t}{(\rho_{s1}c_{s1})_{eff}R_n^2}\sqrt{\rho_{e0}\mu_{e0}V_{max}R_n}\,\dfrac{h_{e0}}{T_{e0}}$. Taking these expressions into account, the fixed values of τ in Fig. 7 correspond to different values of physical time t for different free flow conditions (different values of π_σ). Taking into account the relation $\dfrac{\tau_{eff}}{\tau} = \dfrac{\rho_{s1}c_{s1}}{(\rho_{s1}c_{s1})_{eff}}$ for effective homogeneous body, from the conditions for matching the temperature curves in Fig. 7, for combined and homogeneous bodies we obtain $\tau_{eff} = k\tau$. From this it follows that at $\pi_\sigma = 0.04$, $T_{e0} = 1500$ K for the conditions represented by dashed curves 1 and 2 and at $\pi_\sigma = 0.09$, $T_{e0} = 2000$ K for the conditions represented by dashed curves 3 and 4 in the case where $\tau_{eff} = 0.7\tau$ and $\tau_{eff} = 0.9\tau$.

Thus, the relations obtained make it possible to estimate the nonstationary nature of the formation of the maximum temperature in the vicinity of the critical point on the surface of a spherically blunted conical body at a zero angle of attack, and also make it possible to replace such a combined body by corresponding effective homogeneous bodies.

The distributions of temperature along the surface of combined spherically blunted conical bodies and corresponding homogeneous bodies with effective characteristics are presented in Fig. 8. As expected, in the region where the materials are joined, the temperature of the combined body differs significantly from the temperature in the corresponding region of the homogeneous body. This difference becomes multidirectional in character with time. For stationary conditions, the temperature of the surface of a homogeneous body in this region exceeds the corresponding temperature of the combined body by 100 K. At $\bar{t} = 20$, this temperature is lower than the surface temperature of the combined body steel + AMG by 40–50 K. According to the dashed lines, for $\xi \approx 11$ this temperature on the periphery of the body is lower than T_w for a composite body by 200–250 K. Such is the role of heat transfer in composite and homogeneous materials. Note that in this case it is more convenient to use the dimensionless time $\bar{t}$, rather than multiscale time τ, since the comparison was made at the dimensional time $t = 20$ s.

Let us consider the nonstationary case of flow past a spherically blunted conical body at a nonzero angle of attack. By analogy with work [1], we introduce a nonstationary analog

$$\varphi_{nst} = \frac{\theta_{w1}(\tau, \lambda_s) - \theta_{w0}(\tau, \lambda_s)}{\theta_{w1}(\tau, \lambda_s) - \theta_w(\tau, \lambda_s \to \infty)}, \qquad (7)$$

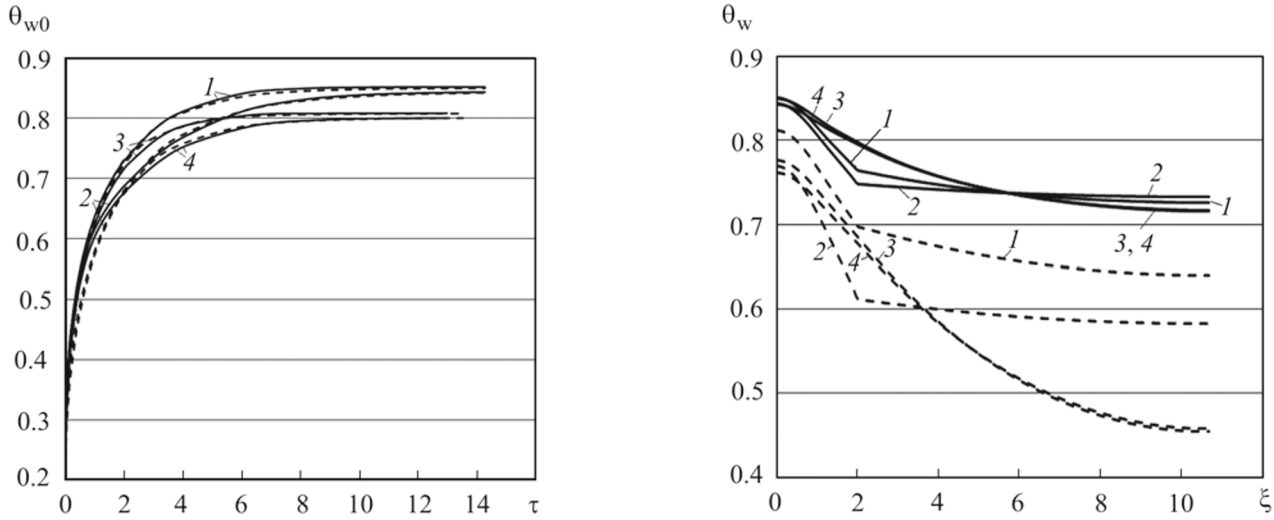

Fig. 7. Temperature at the critical point on the surface of bodies made of steel + AMG (1, 3) and steel + copper (3, 4) and of corresponding effective materials at $\alpha = 0^{o}$, $\pi_{\sigma} = 0.04$ (1, 2), and 0.09 (3, 4), $S_{\text{eff}} = 2.02$ (1), 3.37 (2), 1.77 (3), and 2.05 (4); $\tau_{\text{eff}} = 0.7\tau$ (1, 3) and 0.9τ (2, 4); solid lines, combined materials; dashed lines, effective materials.

Fig. 8. Temperature distributions along the bypass of bodies made of combined materials steel + AMG (1), steel + copper (2), and effective materials (3, 4) at $\alpha = 0^{o}$, $S_{\text{eff}} = 2.02$ (3) and 2.37 (4); solid lines, stationary values; dashed lines, $\tau = t/t_{*} = 20$, $t_{*} = 1$ s.

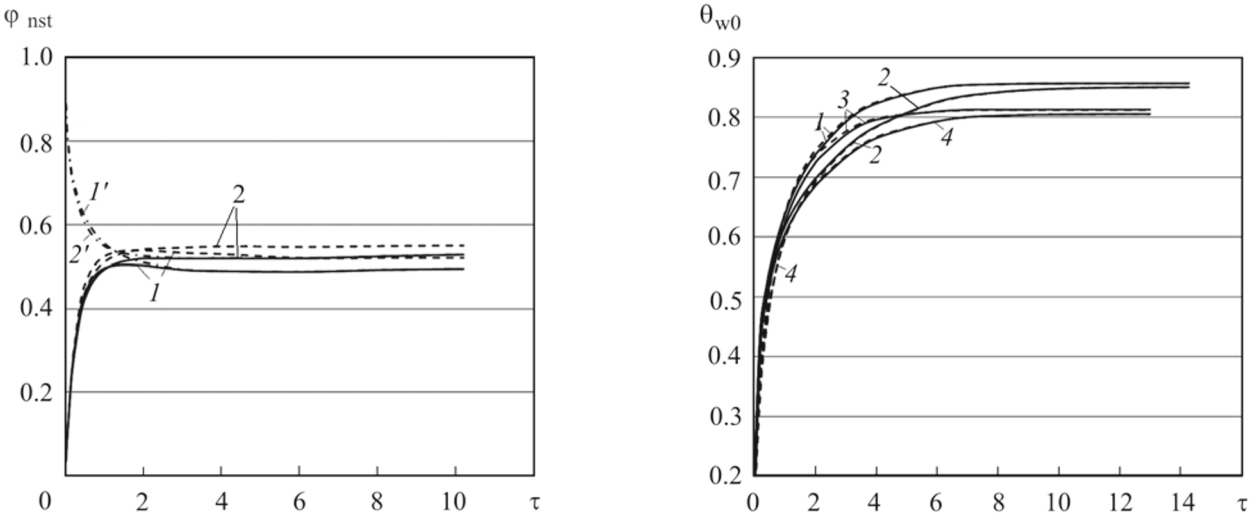

Fig. 9. Dependences of φ_{nst} on time τ for bodies made of combined materials steel + AMG (1) and steel + copper (2) at $\pi_{\sigma} = 0.04$ and $T_{e0} = 1500$ K: solid lines, $\alpha = 0^{o}$; dashed lines; 10.

Fig. 10. Temporal dependences of temperature at the critical point of the bodies made of combined materials steel + AMG (1, 3) and steel + copper (2, 4), obtained by solving the problem in three-dimensional formulation (solid lines) and from approximate formula (9) (dashed lines) at $\alpha = 10^{o}$; 1, 2) = 0.04, $T_{e0} = 1500$ K; 3, 4) 0.09, 2000.

where $\theta_{w1}(\tau, \lambda_s)$ corresponds to one-dimensional calculations. Time dependences of φ_{nst} for various combined bodies are presented in Fig. 9. In this figure, the dashed-dotted lines show the dependence

$$\tilde{\varphi}_{nst} = \frac{\theta_{w,r} - \theta_{w0}(\tau, \lambda_s)}{\theta_{w,r} - \theta_w(\tau, \lambda_s \to \infty)}, \quad (8)$$

which differs greatly from φ_{nst} at the instants of time $\tau < 2$, but does not require the solution of the problem in a one-dimensional formulation. When $\tau \geq 2$, the one-dimensional calculation reaches the values of $\theta_{w,r}$.

Works [1, 10] show the admissibility of equating φ_{nst} and φ_{st} obtained for different angles of attack and different values of π_σ, T_{e0}, and λ_s over the entire range of times. For our case of combined bodies this assumption leads to the expression

$$\theta_{w0}(\tau, \lambda_s) = \theta_{w1}(\tau, \lambda_s) - \varphi_{st}[\theta_{w1}(\tau, \lambda_s) - \theta_w(\tau, \lambda_s \to \infty)]. \quad (9)$$

Let us consider the results of comparing such a numerical solution with the proposed simplification. Figure 10 shows the temperature at the critical point of a spherically blunted conical body as a function of time, obtained as a result of solving the problem under consideration in a three-dimensional formulation and using approximate formula (9) at $\alpha = 10^o$. The dashed curves calculated by expression (9) demonstrate good agreement with the results of the exact solution. As for homogeneous bodies, in expression (9) φ_{st} can be replaced by its value at $\alpha = 0^o$. In this case, the results of the exact and approximate solutions will be very close. At $\tau \geq 2$, as noted above, the solution $\theta_{w1}(\tau, \lambda_s)$ can be replaced by $\theta_{w,r}$.

Thus, during the flow past a spherically blunted conical combined body at an angle of attack in nonstationary conditions, approximate methods of determining the maximum body temperatures can be used based on determining such temperatures in a stationary case and in the limiting cases of $S = 0$ and $S \to \infty$, as well as, if necessary, one-dimensional temperature calculation, $\theta_{w1}(\tau, \lambda_s)$. As expected, these calculations are also valid for effective homogeneous bodies.

Conclusions. The possibility is shown of controlling nonstationary heat transfer in a spherically blunted conical body made of a combined material, when it is immersed in a supersonic gas flow at an angle of attack. For different values of the flow stagnation parameters, the influence of the thermophysical characteristics of the combined material on the maximum temperatures in the region of spherical bluntness of the body is estimated. For the entire time range of the process of interaction of the gas flow with the body until the body reaches the stationary temperature regime, the time periods are estimated in which the use of the combined material is advantageous in relation to the maximum temperatures reached on the surface of the body. Based on calculated data on maximum temperatures on the surface of a combined body in the vicinity of its frontal critical point the technique is suggested for determining the thermophysical characteristics of the so-called effective homogeneous bodies with the same level of the values of T_{w0}. A comparison is made of the initial temperature fields on the surface of effective homogeneous and combined bodies immersed in a flow.

It is shown that the previously obtained dimensionless relations for calculating the maximum surface temperature of a homogeneous body using simplified approaches can be used in the case of a flow past combined bodies. This allows a quick engineering assessment of the maximum body surface temperature at the current time depending on the angle of attack when choosing pairs of materials for the body. The possibilities of highly heat-conductive materials of the conical part of a spherically blunted body to equalize the temperatures of its windward and leeward sides are demonstrated. The results obtained can be used to predict the thermal regime of homogeneous and combined bodies immersed in a flow at different angles of attack.

Acknowledgment. The research was carried out as part of the implementation of the state task of the Ministry of Science and Higher Education of the Russian Federation (Project No. 0721- 2020-0032).

NOTATION

c_s, specific heat of a solid body, J/(kg·K); h and H, static and total enthalpies of gas, J/kg; L, dimensionless thickness of the heat-shielding shell on the lateral surface of the body; M_∞, Mach number of the oncoming flow; n, distance along the outer normal to the body surface, m; p, gas pressure in the boundary layer, N/m^2; q_w, heat flux from the boundary layer, W/m^2; R_n, radius of blunting of the frontal part of the body, m; r, z, and η, radial, axial, and circumferential cylindrical coordinates; r_w, distance from a point on the body up to the axis of its symmetry, m; S, conjugation parameter; St, Stanton number; T, temperature, K; t, time, s; u_e, x component of the velocity of inviscid gas flow on the outer edge of the boundary layer, m/s; V_{max}, maximum velocity of the external gas flow, m/s; V_∞, oncoming gas velocity, m/s; x, length of the arc of

the body generatrix, m; z_0, dimensionless axial coordinate of the rear part of the heat-shielding material in the frontal part; z_c, dimensionless length of the cone; $\alpha = 0^o$; β, taper angle; γ_{eff}, effective exponent of the gas adiabat; ε, emissivity of the body surface; θ, dimensionless temperature; λ_s, thermal conductivity of the body material, W/(m·K); μ, gas viscosity, kg/(m·s); ξ, dimensionless longitudinal coordinate along the media interface, reckoned from the frontal point of the body; π_σ, parameter demonstrating the reradiation of heat from the body surface; ρ, density, kg/m^3, σ, Stefan–Boltzmann constant, W/(m^2·K^4); τ, dimensionless time. Indices: e, external; eff, effective; $i = 1, 2$, parameters related to the frontal and lateral parts of the body, respectively; in, initial; max, maximum; n, nose; nst, nonstationary; r, radiative; s, solid; st, stationary; w, wall; 0, value of the parameter at the stagnation point; ∞, oncoming flow.

REFERENCES

1. V. I. Zinchenko and V. **D.** Gol'din, Problem on conjugate nonstationary heat exchange in supersonic flow over a blunt-nosed cone at an angle of attack, *J. Eng. Phys. Thermophys*., **93**, No. 2, 416–427 (2020).
2. V. I. Zinchenko and V. D. Gol'din, Reducing the maximum surface temperatures in the case of a supersonic flow past a spherically blunted cone, *Teplofiz. Vys. Temp.,* **59**, No. 1, 109–115 (2021).
3. F. Monteverde, R. Savino, M. Fumo, and A. Maso, Plasma wind tunnel testing of ultrahigh temperature ZrB_2–SiC composites under hypersonic reentry conditions, *J. Europ. Ceramics Soc.,* **30**, 2313–2321 (2010).
4. R. Savino, M. Fumo, D. Paterna, A. Maso, and F. Monteverde, Arc-jet testing of ultra-high-temperature-ceramics, *Aerospace Sci. Technol.,* **14**, 178–187 (2010).
5. A. Cecere, R. Savino, C. Allonis, and F. Monteverde, Heat transfer in ultra-high-temperature advanced ceramics under high enthalpy arc-jet conditions, *Int. J. Heat Mass Transf.,* **91**, 747–755 (2015).
6. S. V. Reznik, P. V. Prosuntsov, and K. V. Mikhailovskii, Development of elements of reusable heat shields from a carbon-ceramic composite material. 1. Theoretical forecast, *J. Eng. Phys. Thermophys.,* **92**, No. 1, 89–94 (2019).
7. S. V. Reznik, A. F. Kolesnikov, P. V. Prosuntsov, P. V. Gordeev, and K. V. Mikhailovskii, Development of elements of a reusable heat shield from a carbon-ceramic composite material. 2. Thermal tests of specimens of the material, *J. Eng. Phys. Thermophys*., **92**, No. 2, 306–313 (2019).
8. A. V. Luikov, *Heat and Mass Transfer, Handbook* in Russian], Energiya, Moscow (1972).
9. V. I. Zinchenko, *Mathematical Simulation of Conjugate Heat and Mass Transfer Problems* [in Russian], Izd. Tomsk. Univ., Tomsk (1985).
10. V. I. Zinchenko and V. D. Gol'din, Conjugate problem on nonstationary heat exchange in supersonic flow over a blunt-nosed cone, *J. Eng. Phys. Thermophys.,* **92**, No. 1, 132–140 (2019).